

## VLF and LF signatures of mesospheric/lower ionospheric response to lightning discharges

U. S. Inan, A. Slingeland,<sup>1</sup> and V. P. Pasko

STAR Laboratory, Stanford University, Stanford, California

J. V. Rodriguez

Ionospheric Effects Division, Phillips Laboratory, Hanscom Air Force Base, Massachusetts

**Abstract.** New evidence is presented of disturbances of the electrical conductivity of the nighttime mesosphere and the lower ionosphere in association with lightning discharges. In addition to extensive documentation of the characteristics of a class of events heretofore referred to as early/fast VLF events [Inan *et al.*, 1993], our data reveal a new feature of these events, consisting of a postonset peak that typically lasts for 1-2 s. We also report the observation of short-duration VLF or LF perturbations, in which the amplitude of the subionospheric signal exhibits a sudden change within 20 ms of the causative lightning discharge, and recovers back to its original level in  $< 3$  s. These short-duration events have characteristics similar to the previously observed rapid onset, rapid decay VLF signatures [Dowden *et al.*, 1994]. Both the typical and rapidly recovering events are observed primarily when the causative lightning discharge is within  $\pm 50$  km of the VLF or LF great circle propagation path, indicating that the scattering from the localized disturbance is highly collimated in the forward direction. The latter in turn implies that for the parameters in hand, the transverse extent of the disturbance must be at least  $\sim 100$ -150 km. The measured VLF signatures are compared with the predictions of a three-dimensional model of subionospheric VLF propagation and scattering in the presence of localized ionospheric disturbances produced by electromagnetic impulses and quasi-electrostatic (QE) fields produced by lightning discharges. The rapidly recovering or short-duration events are consistent with the heating of the ambient electrons by quasi-static electric fields, in cases when heating is not intense enough to exceed the attachment or ionization thresholds. When no significant electron density changes occur, the conductivity changes due to heating alone last only as long as the QE fields, typically less than a few seconds. When heating is intense enough so that attachment or ionization thresholds are exceeded, reductions or enhancements in electron density can respectively occur, in which case the medium would relax back to the ambient conditions with the time scales of the local *D* region chemistry, typically 10-100 s.

### Introduction

In recent years, dramatic new evidence of electrodynamic coupling between tropospheric lightning activity and the overlying mesosphere/lower ionosphere has been uncovered, in the form of 'discharges' above the thunderclouds referred to as red sprites and blue jets [Sentman and Wescott, 1993; Lyons, 1994; Sentman *et al.*, 1995; Wescott *et al.*, 1995] and gamma ray bursts of terrestrial origin [Fishman *et al.*, 1994]. However, earlier experimental evidence of direct disturbances of

these atmospheric regions by lightning discharges were in the form of "early/fast" subionospheric VLF perturbations, occurring within  $< 20$  ms of the associated lightning discharges [e.g., Inan *et al.*, 1988, 1993]. Heating and ionization of the lower ionosphere by the electromagnetic impulses (EMPs) released in lightning discharges was initially put forth [Inan *et al.*, 1991] as a possible cause of such events, and a fully kinetic one-dimensional formulation of the EMP-ionosphere interaction has demonstrated that significant ionization can occur, especially at altitudes  $> 85$  km [Taranenko *et al.*, 1993]. Following the video observations of the red sprite type of discharges [Sentman *et al.*, 1995], and especially the clear evidence that the luminous regions extended down to altitudes as low as 60 km, the heating of ionospheric electrons by lightning-induced quasi-electrostatic (QE) fields was put forth as an additional

<sup>1</sup>Now at Qualcomm Inc., San Diego, California.

way in which the mesosphere and the lower ionosphere electrically respond to tropospheric lightning [Pasko *et al.*, 1995].

In this paper, we provide an analysis of an  $\sim 8$ -hour-long episode of lightning-associated VLF and LF events observed in association with a persistent winter storm system in Missouri. The events were observed at Huntsville, Alabama (HU), on the VLF 24.8 kHz NLK signal from Jim Creek, Washington, and on the LF 48.5-kHz signal from Silver Creek, Nebraska. The observed VLF signatures are compared with the predictions of a three dimensional model of VLF Earth-ionosphere waveguide propagation and scattering in the presence of a localized electron density and temperature disturbance produced by heating and ionization changes due to heating of the electrons due to EMP and QE fields.

An illustration of the relevant physical phenomena, the resulting ionospheric disturbances, the measurement of these disturbances by the subionospheric VLF or LF signal, and the two different types of signatures referred to are provided in Figure 1. The data set studied in this paper is rather unusual in the sense that other type of perturbations were also observed in addition to the two types of signatures sketched in Figure 1, albeit at different times and with varying degree of repetition. These included VLF/LF amplitude changes classified as lightning-induced electron precipitation (LEP) events, in which a distinct  $\sim 1$ -s delay between the causative spheric and event onset is observed [Inan *et al.*, 1985, 1988], and heretofore unreported recovery signatures.

For the purposes of this paper, we define a "VLF/LF event" as an amplitude change of magnitude  $\geq 0.2$  dB, lasting for longer than 10 s, typically (but not always) followed by recovery to preevent levels, consistent with previous characterization of similar events [Inan *et al.*, 1993]. The clear exception to this criteria were the newly observed short-duration events, which exhibited discernable ( $\geq 0.2$  dB) amplitude changes, which lasted typically only 1-2 s, clearly longer than the duration of the associated radio atmospheric bursts. The recovery signatures exhibited significant variety, especially those on the 48.5-HU signal.

In interpreting the observed VLF/LF perturbation signatures in terms of electron density or temperature changes, it should be noted that the subionospheric VLF/LF signals propagating in the Earth-ionosphere waveguide generally consist of a summation of a large number of coexisting waveguide modes. Since the attenuation rates and phase velocities of different waveguide modes are comparable, the propagation of these signals over distances of  $< 3000$  km (as in the cases discussed here), and their scattering from localized disturbances, can only be analyzed in the context of a sufficiently general numerical model. For this purpose, we utilize a three dimensional model of VLF propagation and scattering recently developed at Stanford [Poulsen *et al.*, 1993a,b]. This waveguide-mode model is most readily applicable to signals in the frequency range of

$< \sim 30$  kHz, and relatively long ( $> \sim 1000$  km) propagation paths, in which case the signal at the receiver consists of a vector summation of a few modes.

Although the propagation of the LF 48.5-kHz signal can also be modeled, this signal as observed at HU typically consists of a much higher number of waveguide modes [Davies, 1990, section 10.6], due to the higher signal frequency in the LF range and the relatively short propagation path. As a result, the signal amplitude and phase are believed to be highly sensitive to ionospheric disturbances; however, by the same token, quantitative interpretation of the signatures observed on the 48.5-HU path using a waveguide-mode model is considerably more difficult and more critically dependent on the nighttime ionospheric electron density profile. Accordingly, we concentrate in this paper on the quantitative interpretation and modeling of the NLK-HU events, treating the 48.5-HU signatures simply as evidence for the presence of a disturbance. A more general model of VLF/LF propagation and scattering that does not rely on decomposition of the signal into waveguide modes is probably more appropriate for the analysis of the 48.5-HU signal on this short path. In view of the relatively short propagation path, it might also be possible to use a multiple ray theory [Budden, 1961, p.151] to model the propagation and scattering of the 48.5-HU signal.

## General Description of the Experimental Data

The primary VLF/LF data analyzed in this study were acquired at Huntsville, Alabama (HU), where the signals from the 24.8-kHz NLK transmitter in Jim Creek, Washington, and the 48.5 kHz transmitter in Silver Creek, Nebraska, were measured, arriving at HU along great circle paths as shown in Figure 2. Data were typically acquired nightly during  $\sim 0000$ -1200 UT. The case presented here was selected on the basis of an unusually high level of VLF event activity. An earlier case study of lightning-associated VLF/LF events analyzed data from the same VLF/LF transmitter-receiver configuration [Inan *et al.*, 1993].

The National Lightning Detection Network (NLDN) uses a nationwide network of magnetic direction finders to locate individual CG flashes and to record the first stroke peak current (from which the normalized electric field intensity  $E_{100}$  can be derived), polarity and number of strokes [Orville, 1991]. NLDN data for the period 0100-0900 UT on December 15, 1990, are superposed on the great circle signal paths in Figure 2 (pluses represent CG flash locations regardless of polarity), and show a medium-scale thunderstorm center intensify (starting at about 0100 UT) and subsequently fade away by about 0900 UT. Note from Figure 2 that although the center of the storm moved in a northeastward direction into Illinois and Indiana, a thunderstorm cell at the southwestern edge of the storm remained ac-

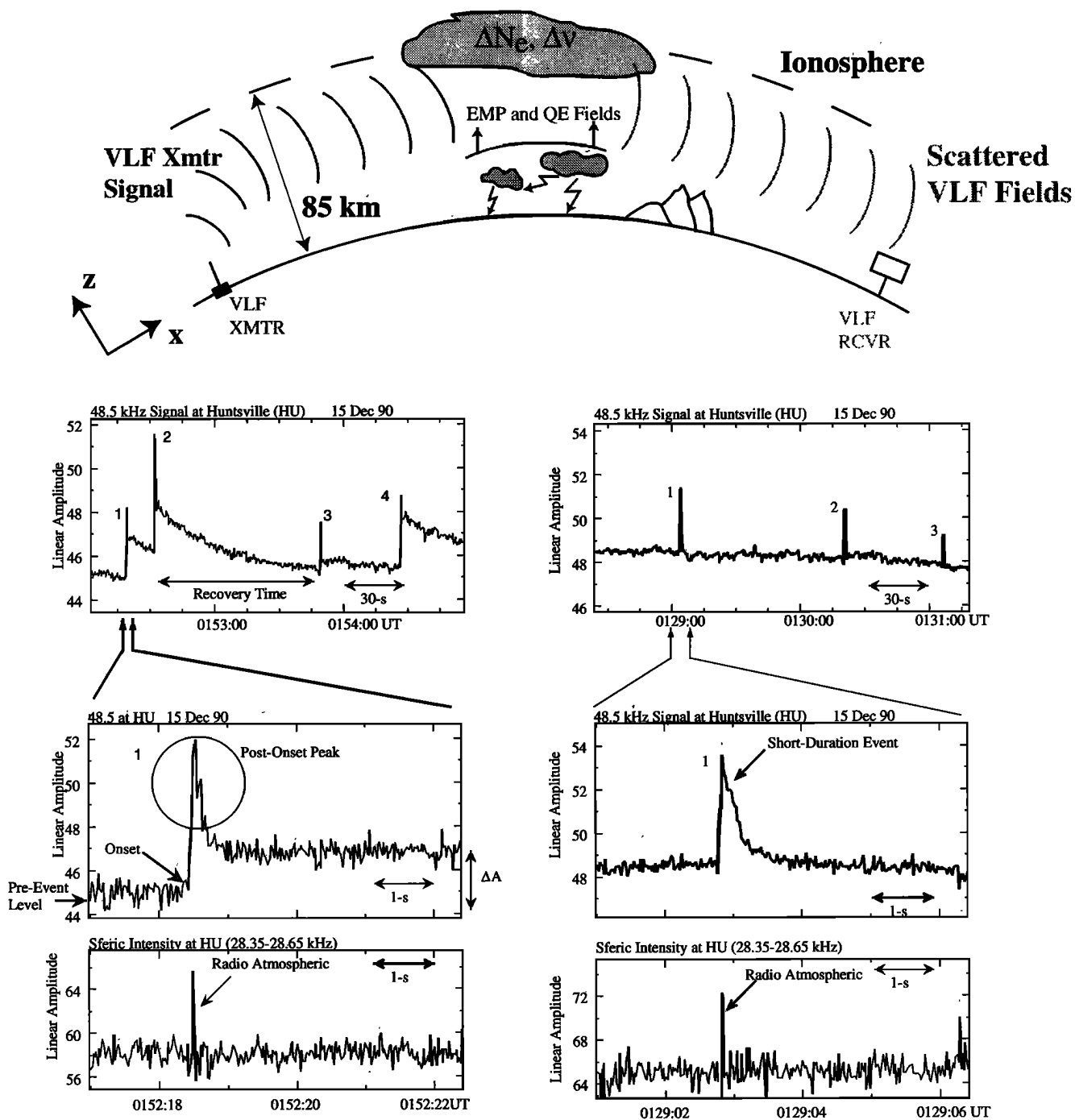


**Figure 1.** The phenomenology of lightning-ionosphere interactions are depicted on the top panel. The set of panels on the left show "early/fast" events (numbered 1-4) exhibiting a post-onset peak (see text). After the event onset, the signal recovers to an intermediate level (marked as  $\Delta A$ ) in  $\sim 1-2$  s, and then recovers to its original level in approximately 10-100 s. The set of panels on the right shows short duration events (numbered 1-3) exhibiting complete recovery to pre-event level in  $\sim 1$  s.

tive within close proximity of the two paths. The active storm centers were well within the area of coverage of the NLDN, where the estimated detection efficiency is 70-80% [Orville *et al.*, 1987]. We note, however, that weaker peak currents (corresponding to  $E_{100} < 3$  V/m)

are not likely to be detected with good efficiency [Idone *et al.*, 1993].

The NLK-HU and 48.5-HU signal amplitudes during 0100-0900 UT are shown in Figure 3. Both signals exhibit relatively slow variations, superposed on which are

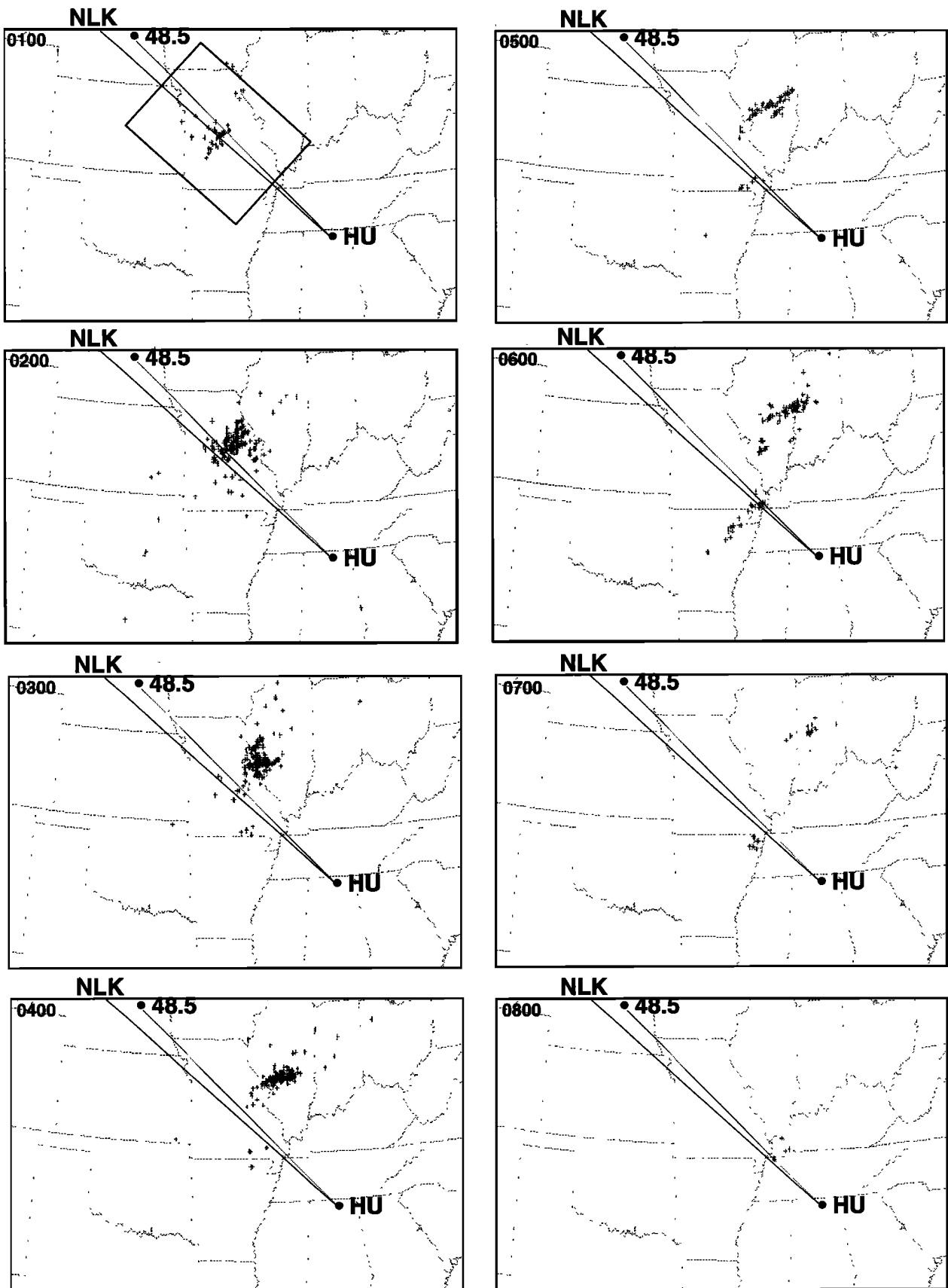


**Figure 2.** Maps showing the location of NLDN CG flashes (both positive and negative CG flashes are represented with a plus symbol) relative to NLK-HU and 48.5-HU VLF paths for 0100 - 0900 UT on December 15 1990. The rectangular region on the top left panel shows a 600x800 km region used in modeling the effects of the ionospheric disturbances on the NLK-HU path, as discussed in a later section.

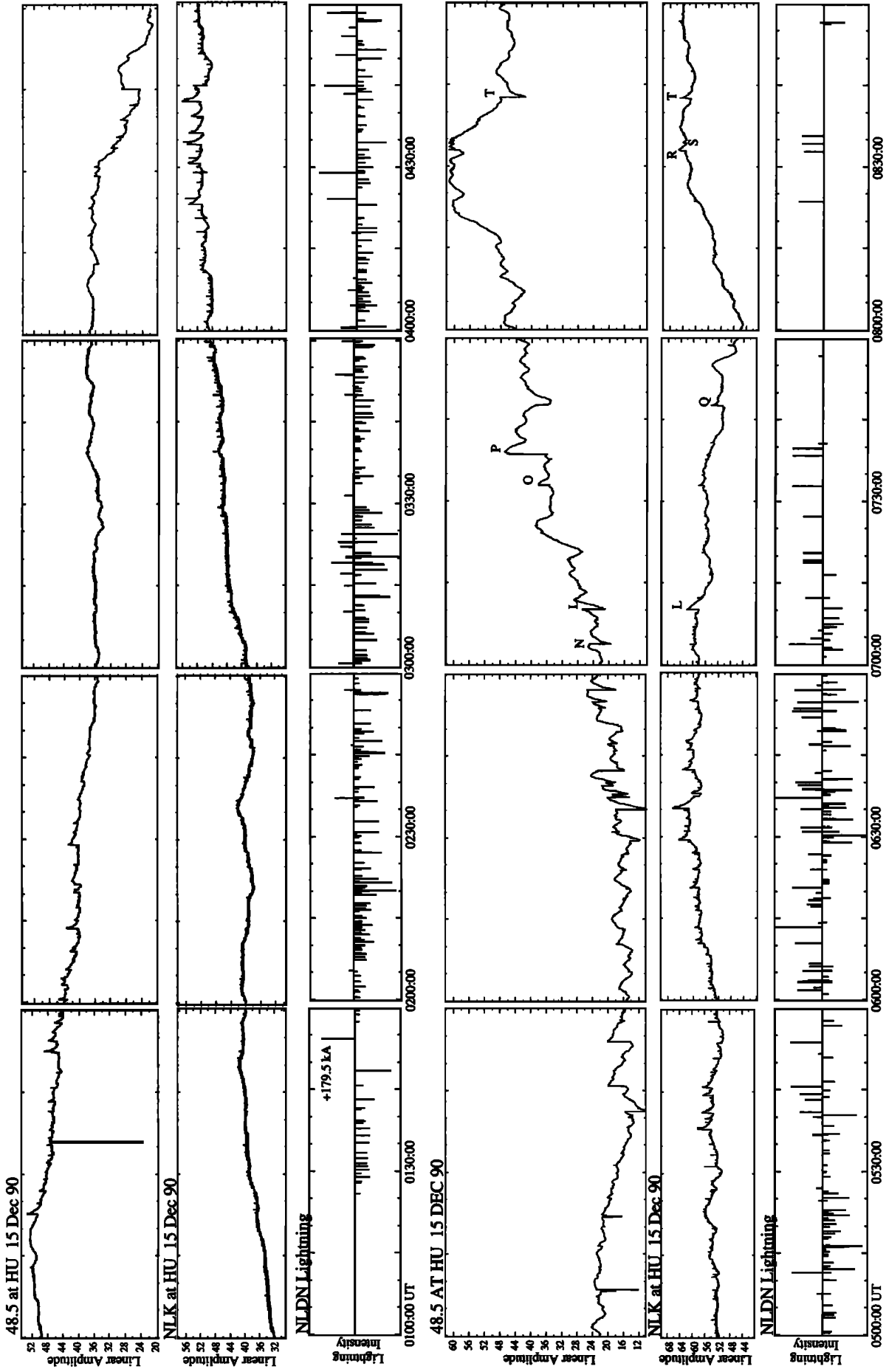


Figure 3. Summary of VLF activity on December 15 1990. Panels show 48.5-kHz LF and NLK (24.8 kHz) VLF signal amplitudes as received at Huntsville, Alabama (HU) from 0100 through 0900 UT. National Lightning Detection Network (NLDN) cloud to ground (CG) lightning data are included, showing the amplitude and time of occurrence of CG lightning flashes.

the so-called 'VLF/LF events', which have the typical signatures of rapid ( $< 1$  s) onsets followed by relatively slow (10-100 s) recoveries. The detection threshold of  $\sim 0.2 \sim dB$  is determined by the background VLF radio atmospheric noise levels. The LF events are observable earlier on the 48.5-HU signal, starting around 0120 UT, whereas on the NLK-HU signal no VLF events are detected until about 0410 UT. Event activity continued on both paths until approximately 0900 UT, when the storm activity subsided. The general character of the event activity on the two signals (48.5-HU and NLK-HU) were quite different, as discussed below. The differences between the two signals can partly be attributed to the relative position of the causative discharges to the propagation paths and the relatively higher sensitivity of the LF signal to changes in ionospheric conductivity.

### LF Event Activity on the 48.5-HU Signal

The events on the 48.5-HU signal exhibited by far a wider variety of temporal signatures, including positive and negative amplitude changes of widely varying magnitudes ( $\sim 0.2$  to 3 dB) and unusual and highly variable recovery signatures. Most of the events on the 48.5-HU signal were of the "early/fast" type [Inan *et al.*, 1993]; in other words, their onsets occurred within  $< 20$  ms of the causative lightning discharges, indicating a direct interaction with the ionosphere as the basic underlying cause. However, a few large events of the LEP type were also observed in later hours (see below for examples), clearly exhibiting the expected [Chang and Inan, 1985; Inan *et al.*, 1988]  $\sim 1$ -s delay between the lightning discharge and event onsets. Among the variety of different signatures, a class of events with unusually rapid recoveries ( $< 2$  s) were observed. This class of events is believed to be signatures of relatively weak lower ionospheric heating by lightning QE fields, in which the average electron temperature remains below the  $\sim 6$ -eV threshold of dissociative attachment of electrons ( $O_2 + e \rightarrow O + O^-$ ) and the higher threshold of ionization (e.g.,  $N_2 + e \rightarrow N_2^+ + 2e$ ). As a result, no significant changes in electron density occur, and conductivity changes due to increased electron temperature last only as long as the driving fields, typically less than a few seconds.

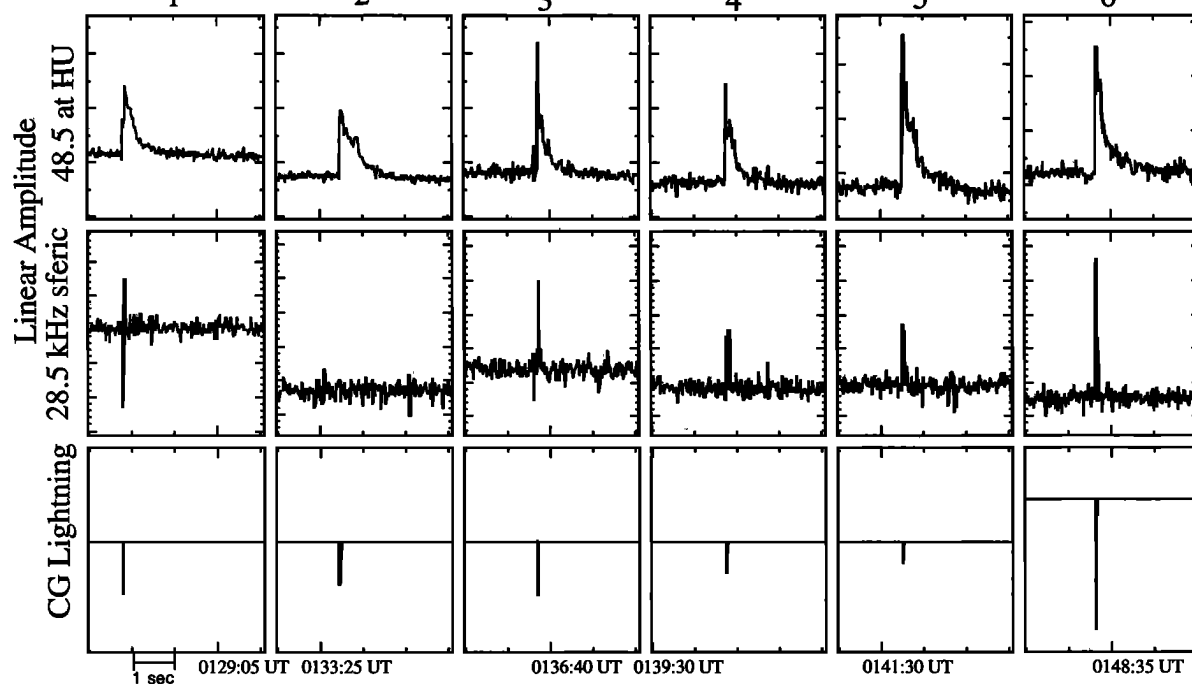
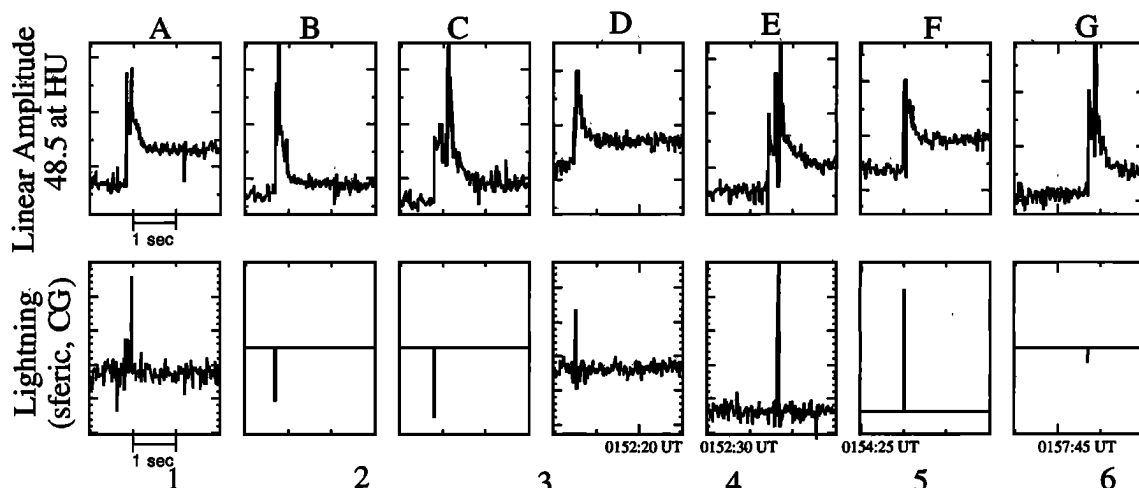
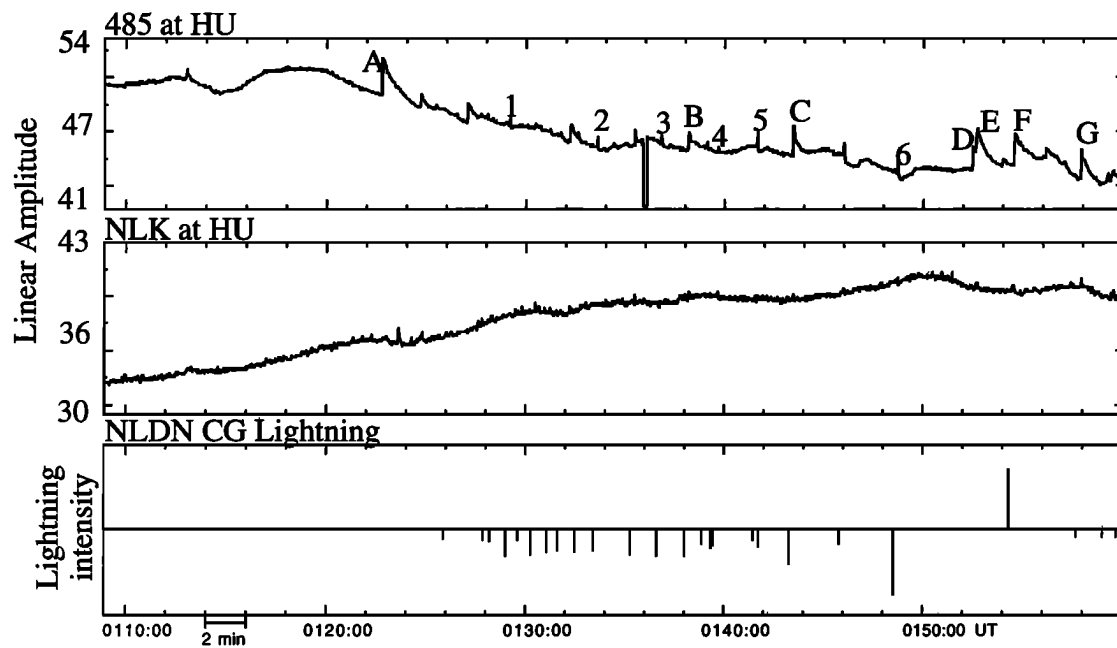
Figure 4 shows an expanded view of the first hour of event activity, namely 0100-0200 UT, when a series of perturbations was observed on the 48.5-HU signal,

without any associated detectable perturbations on the NLK-HU signal. The relationship between causative lightning and the event onsets is illustrated in the high resolution panels showing selected events. Events A - G are common early/fast events. Perturbations were sometimes observed with recorded CG lightning, but were always associated with a sferic. Those events (A, D, E) for which there is no record of CG lightning show a correlation with sferic intensity in the 23.4-0.15 kHz band recorded at Huntsville. Early/fast events have a quick onset delay ( $< 20$  ms) and a fast onset duration ( $< 100$  s) when compared to LEP events. Events A, D, and F clearly show postonset peaks as discussed below, whereas events 1 - 6 are a new type of signature called "short-duration" events, also discussed below. The onsets of the other events (B,C,F,G) are accompanied with CG discharges detected by the NLDN; within the time resolution of our measurement (20 ms) the CG lightning occurs at the same time as the event onsets. The lack of NLDN recorded CG flashes is likely due either to the fact that the network has a detection efficiency of only 70-80% and thus may have missed these flashes, or that these lightning discharges may be intra-cloud (IC) or cloud-to-cloud discharges which are discarded by the NLDN. All VLF/LF perturbations reported in this paper on any of the two paths were accompanied by one or more sferics occurring within the same second as the event onsets; in an overwhelming majority of cases the sferics were isolated single peaks, unambiguously correlated with the event onsets.

**Postonset peaks.** Careful examination of the high resolution signatures of the events in Figure 4 indicates that immediately after the event onset, the signal amplitudes tend to exhibit a relatively rapid recovery to an intermediate level, followed by relatively slow (10-100 s) recovery to pre-event levels. Such a signature is most clearly evident in events A, D, and F but also visible in the others. This type of behavior involving short-duration postonset peaks has been observed and noted in earlier data [Rodriguez *et al.*, 1992a]. Although some of the post-onset peaks could have been produced by the intrusion of the impulsive sferic energy in the frequency band of the signal measured (i.e., the  $24.0 \pm 0.15$  kHz band in the case of Rodriguez *et al.* [1992a], involving the signal from the 24.0-kHz NAA transmitter in Cutler, Maine observed at Wallops Island, Virginia, on July 31, 1987), the fact that such peaks were not

---

**Figure 4.** (Opposite) VLF signatures of early/fast and short duration events. The VLF perturbation events observed on 48.5 and NLK signals and the associated NLDN data for the 0100 UT hour on December 15, 1990 are shown in the top panels. The mosaic of smaller panels show expanded records of selected events, identified, as 1, 2, 3,... or A, B, C,... depending on whether they respectively are short duration or early/fast events. For the expanded records, both the associated CG lightning as recorded by the NLDN, and the sferic intensity in the  $28.5 \pm 0.15$  kHz band as recorded in Stanford receivers are shown. Note that the intense sferics are clearly visible, even though they are superimposed on top of the 28.5-kHz signal from the NAU transmitter located in Puerto Rico [Inan *et al.*, 1988].



observed simultaneously in other narrowband channels led to the suggestion [Rodriguez *et al.*, 1992a] that the postonset peaks were signatures of *D* region heating by the electromagnetic pulse [Inan *et al.*, 1991]. In our case, the postonset peaks are observed on a higher frequency signal so that the intruding sferic energy is relatively lower, and the peaks in question can be seen to clearly last longer than the sferics from Figure 4. These postonset peaks are consistent with the expected response of the LF signal to the combined effects of electron temperature (or collision frequency  $\Delta\nu_{\text{eff}}$ ) and electron density changes ( $\Delta N_e$ ) due to the QE field, which contribute differently to the electrical conductivity to constitute the net signal amplitude change immediately after event onset. However, the temperature change lasts only as long as the QE field (less than a few seconds), so that the amplitude rapidly recovers to a new level as dictated by the conductivity change due only to  $\Delta N_e$ . Any resultant electron density changes (either decreases due to attachment or increases due to ionization), recover at a much slower rate (10-100 s), in accordance with the chemistry of the region [Pasko and Inan, 1994]. This interpretation is discussed in more detail below in the theoretical modeling section.

**Short-duration LF events.** Possibly related to these postonset peaks is a group of events observed during 0100-0200 UT which exhibited only a short-duration peak without any longer lasting signal amplitude changes. Examples of these events (marked 1 through 6) are shown in the lower panels of Figure 4, which also shows the association of the events with VLF sferics and CG lightning. The recovery time of these perturbations is much quicker than that of early/fast events, yet their duration is significantly longer than that of a sferic. These events could be due to electron temperature changes (i.e.,  $\Delta\nu_{\text{eff}}$ ) in cases where the heating of the electrons is not intense enough to induce any ionization changes. These heating-only events were generally more clearly exhibited on the LF 48.5-HU signal than the VLF NLK-HU signal, and were observed primarily during the first 2 hours (0100-0230 UT). All of the short-duration events correlated with CG lightning are correlated with negative CG flashes. Possible interpretations for and implications of these new signatures are provided in the next section. The short-duration events reported here have characteristics similar to the rapid onset, rapid decay VLF events reported by Dowden *et al.* [1994], although our interpretation of these events is substantially different than that of Dowden *et al.* [1994], as discussed in the next section.

Detailed comparison of the occurrence of VLF/LF events of both the long lasting and short-duration types

in comparison with CG lightning location (with respect to the great circle VLF paths) and intensity are provided in the next section. These comparisons indicate that both event types are only detected when the causative CG lightning discharge is within  $\pm 50$  km of the perturbed VLF/LF path. This finding is consistent with the hypothesis that the short-duration events and the postonset peaks are signatures of an ionospheric effect and are not likely to be due to the intrusion of the sferic energy into the signal channel. Note that sferics from discharges outside the  $\pm 50$  km range are also observed in the narrowband channels but are not accompanied with short-duration events. The fact that the short-duration events are not observed in association with lightning outside the proximity range thus constitutes strong evidence of a short-lasting change in the electrical conductivity of the lower ionosphere being induced by the correlated discharges.

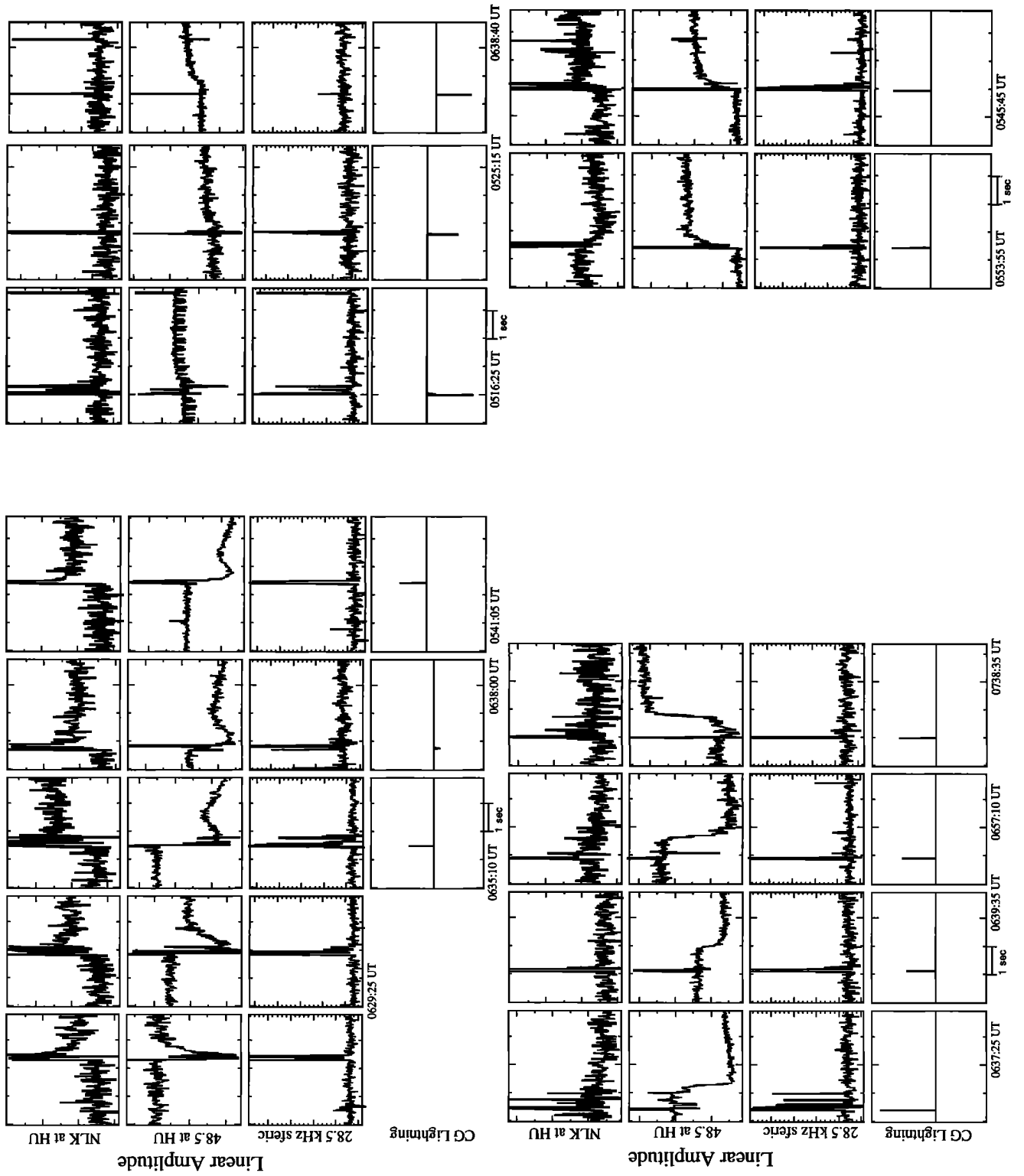
**"Other" VLF events.** A wide variety of perturbation signatures were observed on the 48.5-HU especially in later hours, although the events on NLK-HU were mostly positive and of the early/fast type. Some examples of these are shown in Figure 5. A number of different types of events were observed on 48.5 at HU. The upper left group in Figure 5 shows a series of events where typical early/fast events were seen on NLK at HU, and an assortment of negative events were seen on 48.5 at HU. The bottom left group in Figure 5 shows a number of LEP events (characterized by their onset delay of the order of a second between the causative sferic and the signal perturbation) both positive and negative in amplitude change. These LEP events are associated with stronger flashes 100 - 400 km away from the path. The lower right group of events seem to be short-duration events with negative polarity superposed on an early/fast event. The upper right group of events show a slow increase in the signal intensity for a few seconds following a sferic.

#### VLF Event Activity on the NLK-HU Signal

The character of the VLF events observed on the NLK-HU signal remained similar throughout the period of observation. All except one of these events were positive amplitude changes followed by exponential-like recoveries, similar to previous reports of "early/fast" VLF events [Inan *et al.*, 1988, 1993]. Expanded records of VLF events on the NLK-HU signal are shown in Figure 6, in the same format as Figure 4. The association of event onsets with CG lightning and/or VLF sferics is illustrated in high-resolution panels from selected events. All of the observed NLK-HU events were associated with an NLDN detected CG lightning discharge

**Figure 5.** (Opposite) Variety of VLF events observed on 48.5 and NLK signals at HU. Each panel shows expanded records of events, showing the amplitudes of the 48.5-HU and NLK-HU signals, the sferic intensity of the  $28.5 \pm 0.15$  kHz band, and CG lightning data as available.





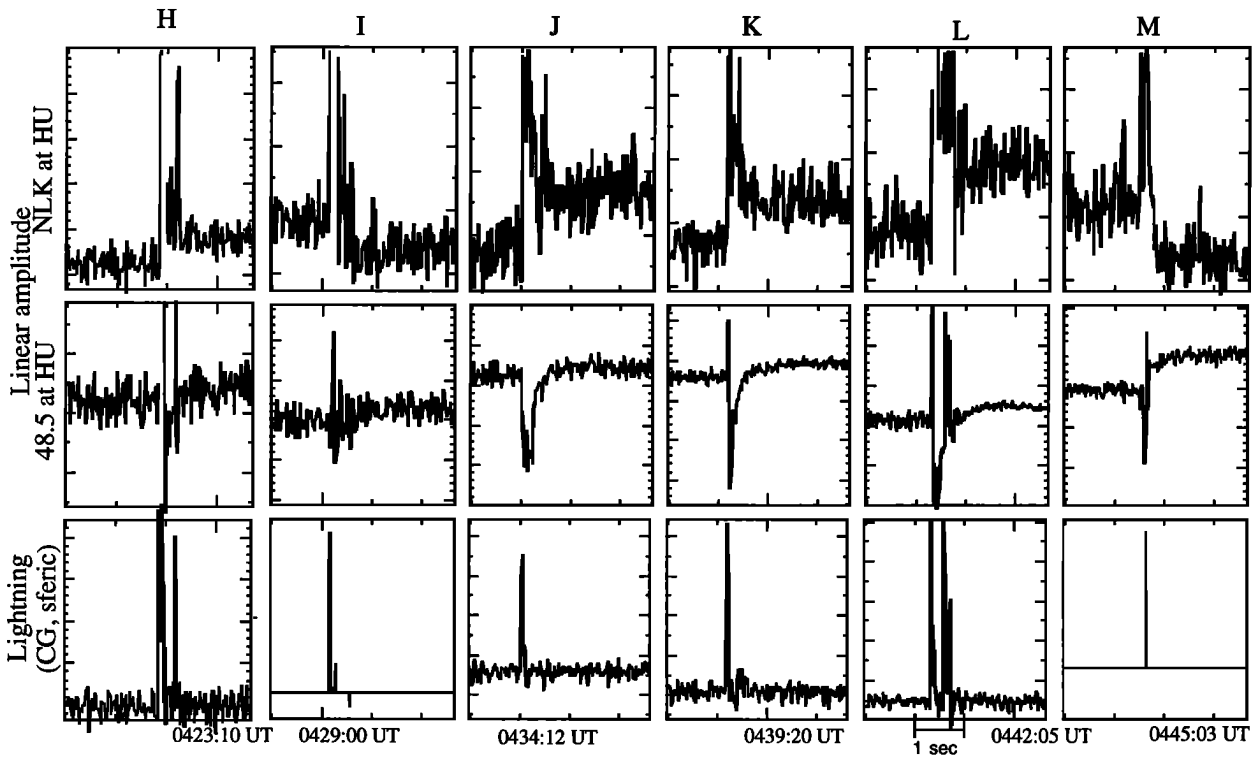
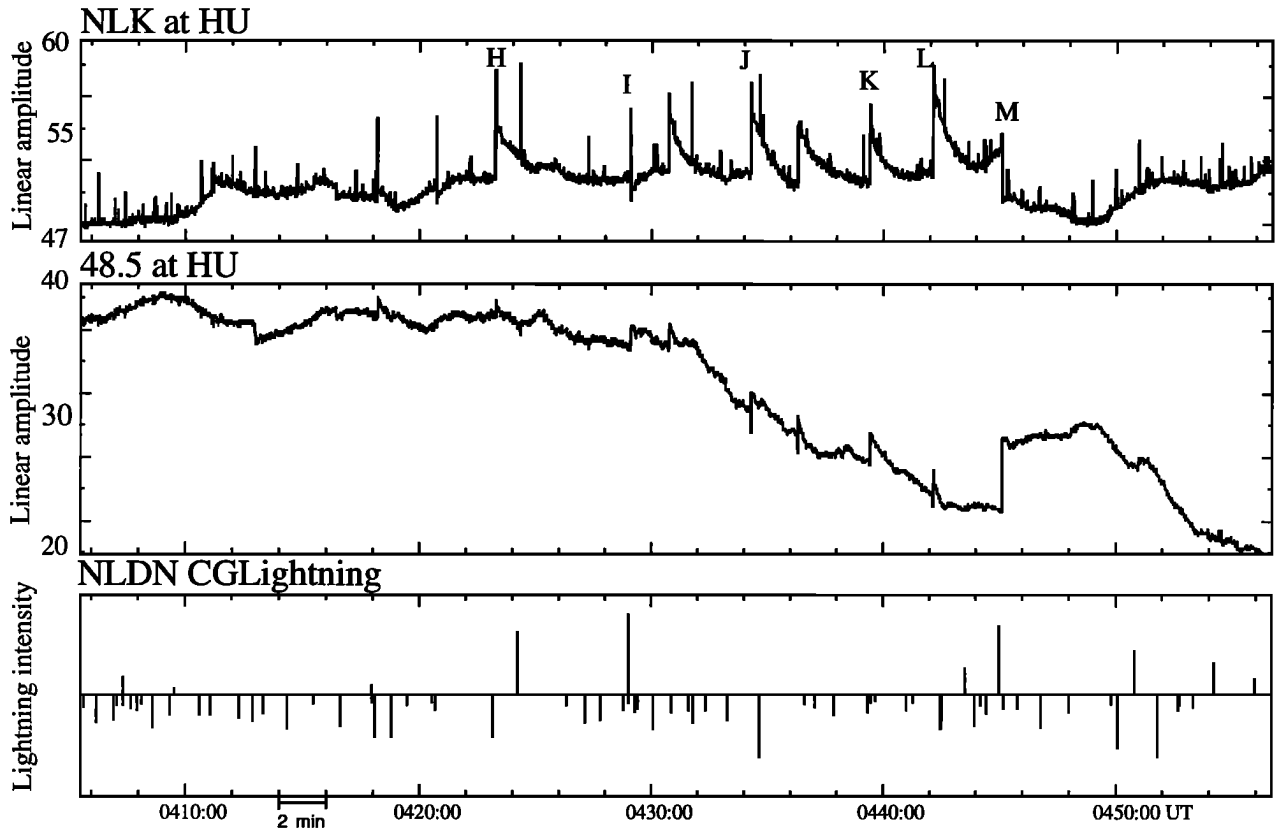


Figure 6. Top panels show data for approximately a 1-hour period with early/fast events labeled H through M. The bottom set of panels show the events on an expanded timescale. The bottom panel shows lightning correlation with NLDN CG data if available (NLDN records only approximately 70% of CG strokes), otherwise with sferic intensity in the  $28.5 \pm 0.15$  kHz band. The format is identical to that of Figure 4.

and/or a VLF radio atmospheric, occurring within  $< 20$  ms of the event onset. The onset of the one event with a negative amplitude change (event M at  $\sim 0445$  UT, see Figure 6) occurred within 20 ms of a large positive CG discharge. In contrast to the 48.5-HU signal, no events with delayed onsets (i.e., LEP events) were observed on the NLK-HU signal.

Closer examination indicated that many of the NLK-HU amplitude changes also exhibited a sharp postonset peak prior to the relatively slow (10-100 s) recovery to pre-event levels. However, due to the intense spheric energy in the NLK band ( $24.8 \pm 0.15$  kHz), it was not always possible to definitively rule out the contribution to these postonset peaks of the intrusion of spheric energy into the narrowband channel. However, in at least some of the cases (see events K and L in Figure 6), the postonset peaks lasted clearly longer than the spherics and exhibited a rapid recovery to an intermediate level in a manner similar to the 48.5-HU events discussed in the previous subsection. The absolute amplitudes of the events ranged between 0.1 to 0.7 dB, as shown in a histogram format in Figure 7. The amplitudes shown here are  $\Delta A$ , or the difference between the preevent level and the signal level at the termination of the postonset peak, as illustrated in Figure 1.

Note that many of the NLK-HU events shown in Figure 6 were also detected on the 48.5-HU signal, albeit with more complicated signatures. On the contrary, none of the 48.5-HU events (neither the heating-only nor the heating-plus-attachment events) which occurred during the 0100-0200 UT hour (Figure 3) were detected on NLK-HU. This result is likely due to the different sensitivity of the VLF and LF signals to ionospheric conductivity changes.

### Comparison of VLF Events With CG Lightning Intensity and Location

Past work on "early/fast" VLF/LF signatures [Inan *et al.*, 1993] has indicated that events were detected only when the causative lightning discharges were located within  $\sim \pm 50$  km of the great circle propagation path. The present larger data set allows us to check the validity of this finding. Figure 8 shows the dependence of the VLF/LF event-CG lightning association on the intensity of the CG flashes expressed as the normalized (to 100 km distance) electric field in Volts per meter ( $E_{100}$ ) and shortest great circle distance from the recorded CG location to the 48.5-HU and NLK-HU paths. For both paths, positive (negative) distance values correspond to northeast (southeast) of the path. The short-duration events observed on 48.5-HU during 0100-0230 are separately indicated. In comparing the VLF/LF event occurrence with NLDN CG lightning data it is important to keep in mind that the coverage efficiency of the NLDN is only 70-80% [Orville *et al.*, 1987]. Ionospheric disturbances (and hence VLF/LF events) may well have been produced by intracloud

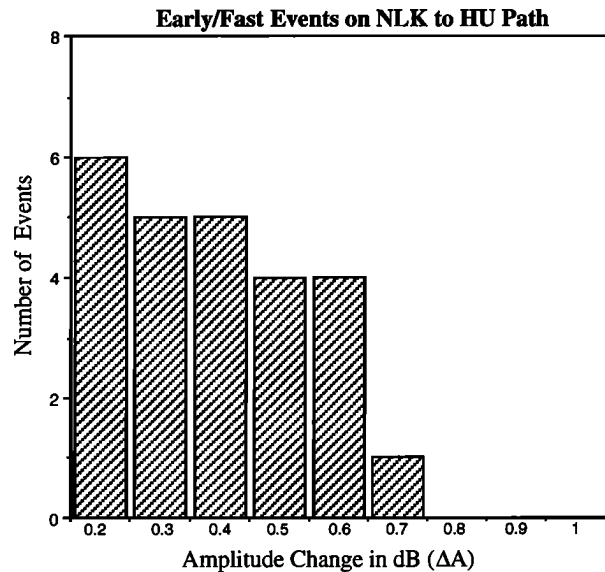


**Figure 7.** Distribution of the magnitude of amplitude perturbations ( $\Delta A$ ) of the early/fast VLF events measured on the NLK-HU signal.

lightning discharges from the same storm center, which are not recorded by NLDN.

We see from Figure 8 that during the first hour (0100-0200 UT), all of the CG flashes within  $\pm 50$  km of the 48.5-HU path led to either short-duration events (indicated by triangles) or the more typical early/fast LF events (circles). No corresponding events are observed on the NLK-HU signal, even though the CG flashes are within close proximity of this path. The correspondence between LF events and CG lightning is similar during 0200-0300 UT, although some CG flashes within  $\pm 50$  km are not accompanied by LF events. Once again, no VLF events are observed on the NLK-HU signal; however, the storm center has moved substantially north of this path so that there are few flashes within  $\pm 50$  km of this path. It is also interesting that some relatively intense CG flashes (e.g., with  $E_{100} \simeq -40$  to  $-50$  V/m) within the  $\pm 50$  km range have not produced VLF/LF events, indicating that characteristics of the lightning discharges other than the peak electric field as recorded by NLDN may sometimes be a more important measure of the effectiveness of the lightning-ionosphere interaction.

From Figure 3, we note that the VLF activity on the 48.5-HU signal subsides during 0300-0400 UT, with literally no VLF events observed during this hour. Examination of Figure 8 indicates that this result is simply due to the fact that the lightning activity was entirely outside the  $\pm 50$  km proximity region of the two paths. During the next hour (0400-0500 UT), only two CG flashes were recorded by NLDN to occur close to the paths. The  $\sim 45$  V/m flash occurring at  $\sim 0445:03$  UT produced events on both the 48.5-HU and NLK-HU signals, while the much weaker CG flash did not.

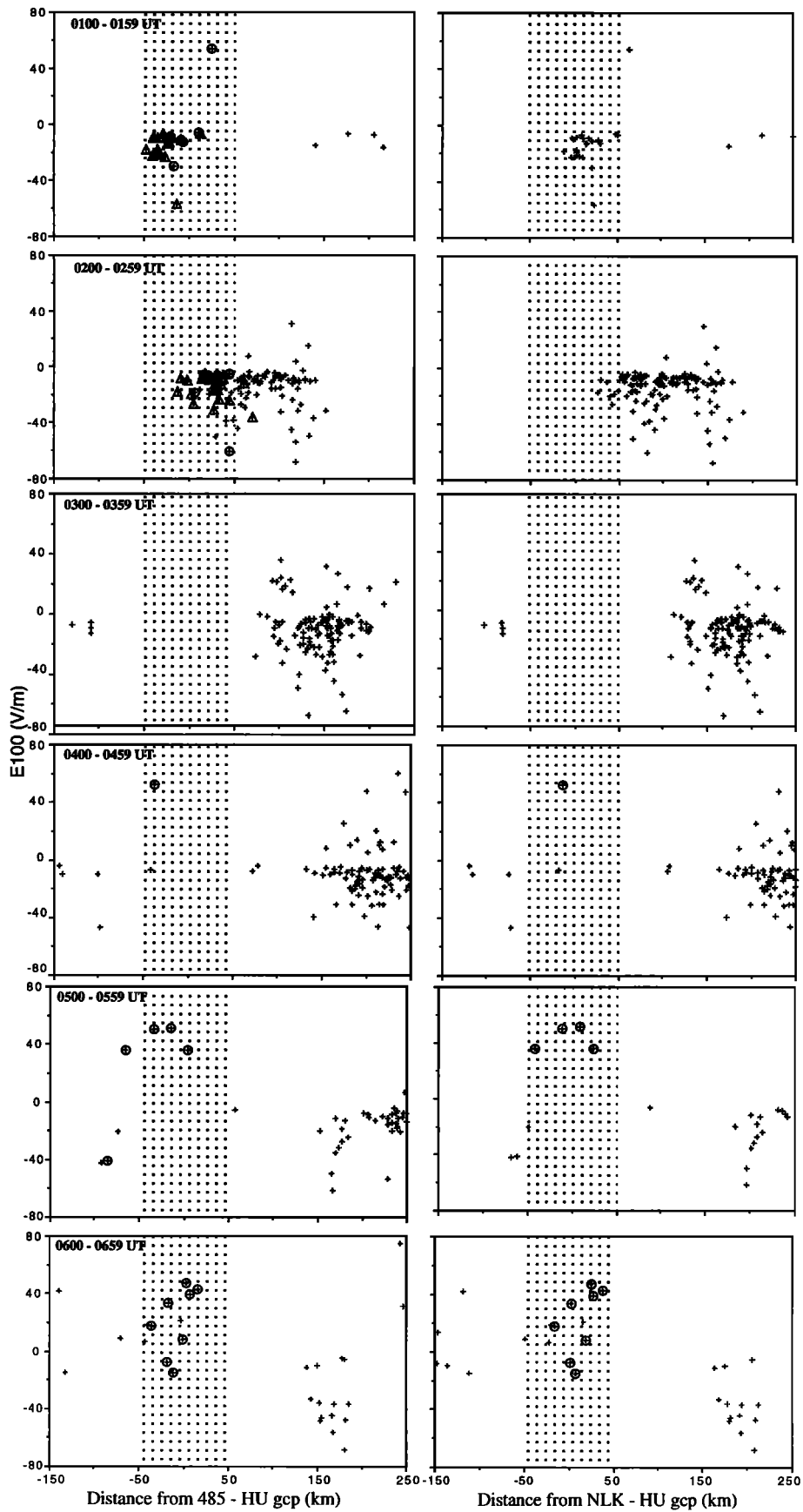


**Figure 8.** The distribution of CG lightning (pluses) in terms of flash intensity at 100 km distance ( $E_{100}$ ), with  $E_{100} < 0$  indicating a negative flash, and distance from the VLF and LF paths. Flashes which are correlated with early/fast VLF events are marked with a circle. Flashes correlated with short-duration events are marked with a triangle. The series on the right is with reference to the NLK-HU VLF path, and the series on the left with respect to the 48.5-HU LF path.

The VLF/LF signature corresponding to this very large flash was unusual in many respects. This event, marked M in Figure 6, was observed as a negative amplitude change on NLK-HU (while all the other events during this hour were positive changes). On the 48.5-HU signal, the event was observed as a positive change of magnitude three times larger than any other event during this hour and also exhibited unusual recovery signatures lasting for almost 10 mins. One other NLK-HU event labeled I was associated with a CG flash which occurred at a distance of  $\sim 236$  km from the path (i.e., outside the range of Figure 8). We note from Figure 6 that many other events were observed on the NLK-HU path (and fewer on the 48.5-HU signal) during this period, indicating that they may have been produced by CG flashes missed by the NLDN or intracloud flashes.

During the 0500-0600 UT period, all four of the CG flashes within  $\pm 50$  km of the NLK-HU path produced perturbations; these flashes were all quite intense positive discharges with  $E_{100} > 35$  V/m. All four of the CG flashes also produced associated events on the 48.5-HU signal. A relatively large ( $E_{100} \simeq 40$  V/m) negative flash occurring outside the  $\pm 50$  km range has also produced a perturbation on the 48.5-HU signal, with no detectable perturbation of the NLK-HU signal, even though the CG flash was closer to this path. Once again, we see the differences in sensitivity of the VLF/LF paths to ionospheric disturbances.

A higher rate of CG lightning activity close to the paths during 0600-0700 UT apparently leads to a higher rate of VLF/LF events observed on both signals. We see from Figure 8 that 8 out of 10 CG flashes within  $\pm 50$  km of the paths led to VLF/LF events. Furthermore, we note that the recorded intensities of these flashes ranges from  $-10$  V/m to  $> +40$  V/m. The distribution of CG flash positions in this and the previous hour was such that no large positive CG flashes occurred immediately outside the  $\pm 50$  km range.

Only a few events were observed after 0700 UT when the storm activity subsided, although some of the most interesting and complex LF responses were observed during this period. During 0700-0800 UT, four CG flashes were recorded within 44, 41, 49, and 41 km of the NLK-HU path with intensities of  $E_{100} = 18, 6, 48,$  and  $5$  V/m, respectively. Of these, the  $\sim 48$  V/m flash produced event O on 48.5-HU as shown in Figure 9. Two other VLF events observed during this period, namely events L and Q, did not have associated CG flashes but were typical early/fast events.

None of the NLDN recorded CG lightning was within  $\pm 50$  km of the 48.5-HU path during 0700-0800 UT. However, strong CG discharges at greater distances produced a variety of signatures, as displayed in Figure 9. Event N was a typical negative amplitude LEP event associated with a 53-V/m flash at a distance of 105 km. Event L had a very similar signature, although no CG flash was recorded by NLDN; nevertheless, a clear radio atmospheric was observed as shown in Figure 9.

(Note that the corresponding event L on NLK-HU is a typical early/fast event.) The signature of event O on the 48.5-HU signal appears to be a superposition of an initial rapid recovery (much like the short duration events discussed in connection with Figure 4) followed by a positive amplitude LEP event. This event was associated with a 48 V/m CG flash which occurred at a distance of 68 km from the path. The following three events shown in Figure 9 included two negative amplitude short duration events and a gigantic positive amplitude LEP event which was associated with a 48 V/m CG flash at a distance of 96 km.

Even fewer VLF/LF events were observed during 0800-0900 UT. The only two flashes within  $\pm 50$  km of the NLK-HU path both caused typical early/fast events, marked R and S in Figure 3, with event R also being observed on the 48.5-HU signal. The single outstanding event T observed at 0842:34 UT was also an early/fast event, with the event onsets on both NLK-HU and 48.5-HU occurring within  $< 20$  ms of an intense radio atmospheric.

### Summary of Experimental Data

The salient aspects of the data presented above can be summarized as follows:

1. Early/fast VLF/LF perturbations are observed on both the 48.5-HU and NLK-HU signals, with the amplitude changes on NLK-HU varying between 0.2-0.7 dB and slower recoveries lasting  $\sim 10$  s to a few minutes.
2. Most VLF/LF events exhibit a postonset peak lasting for 1-2 s, substantially longer than sferics but much shorter than that expected for aeronomic recovery of ionospheric disturbances at 60-90 km altitudes [Pasko and Inan, 1994].
3. A different type of VLF/LF signature, called short-duration events, is observed; these events are similar to the post onset peaks but are not followed by a slow recovery. These events were observed when the storm center, constituted by CG flashes of primarily negative polarity, was within  $\pm 50$  km of the 48.5-HU path. The temporal signatures of these short-duration events are similar to those of the previously reported rapid onset, rapid decay events [Dowden *et al.*, 1994].
4. Both negative and positive CG flashes are seen to lead to VLF/LF events, with the causative flash intensities ranging from  $-10$  V/m to  $\sim 50$  V/m.
5. A large percentage of all CG flashes occurring within  $\pm 50$  km of the path was found to lead to VLF/LF events. Only one example was found (event I in Figure 6) of a very intense flash occurring at a distance of  $\sim 236$  km which occurred at the time of a detectable event on the NLK-HU signal.
6. A range of unusual signatures were observed, including nonexponential recovery signatures on the 48.5-HU signal and one case of an unusually long lasting ( $\sim 10$  mins) recovery (event M in Figure 6).

## Theoretical Modeling

The VLF and LF data shown above provide strong evidence that the electrical conductivity of the mesosphere and the lower ionosphere above thunderstorms is modulated by the energy released in lightning discharges. Two different means by which electron density and temperature changes can occur have recently been identified, involving heating and ionization of the free electrons by (1) electromagnetic pulses (EMP) radiated by lightning discharges [Inan *et al.*, 1991; Taranenko *et al.*, 1993], and (2) Quasi-electrostatic (QE) fields produced by lightning discharges [Pasko *et al.*, 1995]. The EMP from lightning typically lasts only a few hundred microseconds which is also approximately the duration of time during which the electron temperature remains elevated. In view of the fact that our VLF/LF data are sampled at 20 ms intervals, it is not likely that electron temperature changes due to EMP would be detectable in our data. The EMP-induced heating does lead to ionization [Inan *et al.*, 1991; Taranenko *et al.*, 1993]; however, most of the disturbances are predicted at altitudes >85 km, less likely to affect the VLF or LF signals, for which the nighttime reflection height is  $\sim 85$  km [Wait and Spies, 1964]. Accordingly, we limit our attention in this paper to heating and ionization by QE fields, the disturbances from which lie largely below 85 km altitude [Pasko *et al.*, 1995]. We consider ionospheric disturbances that are expected to be produced by the QE heating mechanism under a variety of conditions and evaluate the scattering of the subionospheric VLF 24.8-kHz NLK signal from such disturbances.

### Heating of the Ambient Electrons by QE Fields Ionization Changes and Optical Emissions

The recently developed self-consistent model [Pasko *et al.*, 1995] of heating of lower ionospheric electrons by QE fields can be readily used to determine the spatial size and temporal variations of the resultant electron temperature and density changes, under any given set of input conditions. The important inputs to the model are (1) the ambient ion conductivity and electron density models, (2) the magnitude ( $Q$ ) of the charge transferred (by a CG lightning discharge) and the time ( $\tau$ ) over which the charge is transferred, and (3) the altitude of the cloud charge removed. None of these parameters are available to us directly for the data set in hand, except for the fact that the NLDN recorded lightning intensity (or peak current  $I_p$  [e.g., Idone *et al.*, 1993]) does imply some restrictions on  $Q$  and  $\tau$ .

In the context of the QE model, the lightning discharge is taken to consist of two stages [Pasko *et al.*, 1995]. During a predischage stage with duration  $\tau_o$ , charge  $Q_o$  slowly (hundreds seconds) accumulates in a thundercloud. The second stage is the discharge itself, during which the thundercloud charge is quickly and completely removed from the thundercloud during time

$\tau$  which is usually of order of several ms. Mathematically the continuous charge dynamics in thundercloud can be represented in the form:

$$Q(t) = Q_o \frac{\tanh(t/\tau_o)}{\tanh(1)}, \quad 0 < t < \tau_o$$

$$Q(t) = Q_o \left[ 1 - \frac{\tanh(t/\tau)}{\tanh(1)} \right], \quad \tau_o < t < \tau_o + \tau$$

$$Q(t) = 0, \quad \tau_o + \tau < t$$

Note that the choice of the functional variation as  $\tanh(\cdot)$  is rather arbitrary but is not critical to any of the discussion in this paper.

For this particular assumed functional dependence of  $Q(t)$  the amplitude of the peak current at  $t = \tau_o$  can be calculated as

$$I_p = \frac{dQ}{dt} = \frac{Q_o}{\tau \tanh(1)}, \quad t = \tau_o$$

Having calculated  $I_p$ , the value of the electric field at a distance of 100 km from the lightning discharge can be found as [Orville, 1991]

$$E_{100} = \frac{I_p v}{2\pi D \epsilon_o c^2}$$

where  $c$  is speed of light in free space,  $\epsilon_o$  is dielectric permittivity of free space,  $D = 10^5$  m,  $v = 1.5 \times 10^8$  m/s.

For example,  $E_{100}=75$  V/m corresponds in this model to a peak current of  $I_p=270$  kA and a total charge removed in lightning of  $Q_o=200$ C, if we assume  $\tau=1$  ms, a reasonable value based on experimental data [Uman, 1987, pp. 124, 199]. We note that the duration of the lightning discharge  $\tau$  as well as the functional time dependence of charge removal  $Q(t)$  as given above are not available from measurements provided by NLDN. Nevertheless, these parameters are crucially important for the correct estimation of the charge removed in the lightning discharge and thus in modeling the corresponding heating and ionization changes in the lower ionosphere.

Another important input into the QE model is the ambient ion conductivity profile, which determines the relaxation time for the QE field and thus the amount of heating for given values of  $Q$  and  $\tau$ . In the following analysis, we show results for an ion conductivity as given by Dejnakarindra and Park [1974]; in cases of lower ion conductivity, such as that reported by Holzworth *et al.* [1985], similar heating of the ambient electrons and the resultant ionization changes would occur for lower values of  $Q$ .

Figure 10 shows the altitude distributions of lower ionospheric electron density  $N_e$ , effective electron collision frequency  $\nu_{\text{eff}}$  and optical emission intensity of first positive band of  $N_2$  for  $Q = 25, 150$  and  $300$  C. In all cases, it was assumed that charge  $Q$  was removed from 10 km altitude in  $\tau=1$  ms. We note that signif-

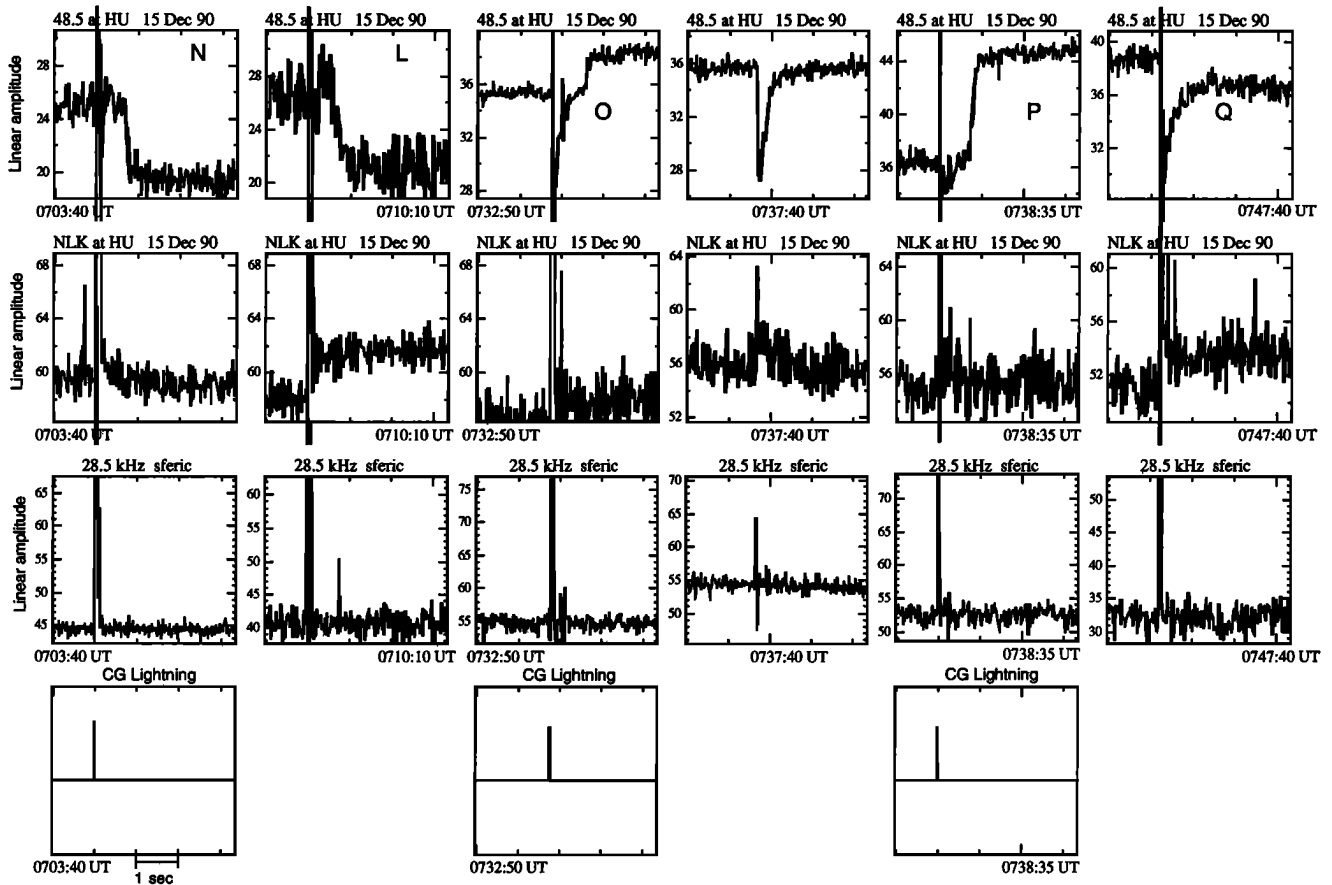


Figure 9. VLF signatures observed on 48.5 and NLK signals at HU for 0700-0800 UT on December 15, 1990. Sferic and NLDN (if available) data are also shown for reference, in the same format as Figures 4 and 6.

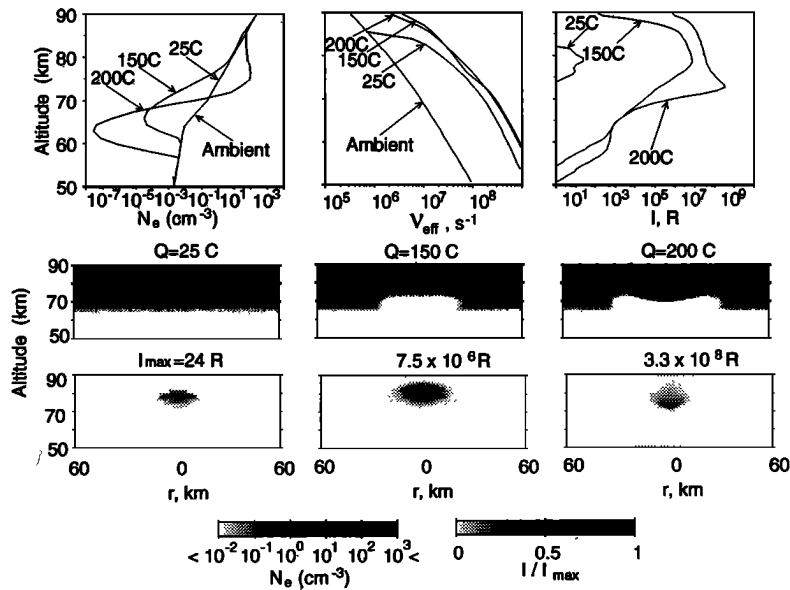


Figure 10. Results of a two-dimensional QE model [Pasko et al., 1995] calculations of the lower ionospheric electron density  $N_e$ , effective electron collision frequency  $\nu_{eff}$  and optical emission intensity of first positive band of  $N_2$  for values of thundercloud charge  $Q$  removed in a cloud-to-ground discharge of  $Q=25, 150, \text{ and } 200$  C.

icant heating occurs even for  $Q = 25$  C, but that no appreciable ionization changes or optical emissions are expected.

For  $Q = 150$  C, the heating is sufficiently high (i.e., the temperature of a large number of electrons is elevated to near  $\sim 6$  eV) to lead to significant depletion in electron density due to dissociative attachment ( $O_2 + e \rightarrow O + O^-$ ). Since the elevated electron temperatures which can cause measurable optical emissions persist for only 1-2 ms, the instantaneous optical emission intensity given in Figure 10 would be reduced by a factor of  $\sim 10$  when averaged over a typical 16-ms video frame used in red sprite observations [Sentman *et al.*, 1995]. Furthermore, the red filter used has a sharply defined spectral range of 550 to 700 nm [Wescott *et al.*, 1995], while the first positive band ranges from 700 nm to 1700 nm, meaning that the reported observations measure only a few percent of the total optical energy released in the  $N_2$  first positive band. Accordingly, the value in Figure 10 of 7500 kR for the 150 C case would be observed as a  $< 10$  kR emission using the techniques of Sentman *et al.* [1995] and Wescott *et al.* [1995]

For  $Q = 200$  C, on the other hand, attachment is even more effective at the lower altitudes, leading to an almost complete depletion (i.e., reduction from  $\sim 10^{-3}$   $cm^{-3}$  to  $\sim 10^{-7}$   $cm^{-3}$ ) of density in the altitude range of  $\sim 55$  to  $\sim 67$  km. However, an ionization increase by as much as a factor of  $\sim 10^2$  occurs in the 70-80 km altitude range. The resultant ionization profile shown in Figure 10 represents a substantial modification of the ambient profile, and would be expected to have a significant effect on the amplitude and phase of subionospherically propagating VLF signals. However, we note that the transverse size of the disturbed region is relatively small, being  $\sim 50$  km in extent, as can be seen from Figure 10. In terms of optical emission intensities, the peak instantaneous intensity of  $\sim 3 \times 10^5$  kR would be observed as  $\sim 300$  kR as measured in the Sentman *et al.* [1995] and Wescott *et al.* [1995] experiments, in the upper range of observed red sprite intensities [Sentman *et al.*, 1995]. Note that the production of enhanced ionization by the QE heating process substantially increases the optical output [Pasko *et al.*, 1995]. In other words, readily observable red sprites would have occurred if the CG discharges involved removal of  $Q = 200$  C in  $\tau = 1$  ms. On the basis of our earlier discussion, these parameters would correspond to  $I_p = 270$  kA or  $E_{100} = 75$  V/m; we further note from Figure 8 that all of the CG flashes in the thunderstorm under study had intensities  $E_{100} < 50$  V/m. In other words, for a discharge time of  $\tau = 1$  ms, thundercloud altitude of 10 km, and in the context of the QE model, the CG flashes in the December 15, 1990, thunderstorm were likely characterized by charge removals of  $Q < 150$  C, and led to the production of relatively weaker ( $< 10$  kR in the 550-700 nm band over 16-ms frame times) red sprites, most likely below detectable levels.

### VLF Signal Amplitude Changes

To determine the amplitude and phase changes on the NLK-HU signal we use a three-dimensional model of VLF Earth-ionosphere waveguide propagation and scattering [Poulsen *et al.*, 1993a,b]. This model was based on the earlier work of Wait and Spies [1964] and neglects conversion between different waveguide modes under the disturbance on the basis that the lateral variation of the disturbance is small. For this analysis, we consider a rectangular region of size  $600 \times 800$  km centered around the storm location at 0100 UT as shown in Figure 2. Since lightning discharges at various points within such a range were found to cause VLF perturbations, we calculate the expected amplitude changes  $\Delta A$  as a function of disturbance location at different points transverse and along the path. As in other cases [Poulsen *et al.*, 1993a],  $\Delta A$  is nearly independent of position along the path, but depends sensitively on the transverse distance of the disturbance center from the path. Figure 11 shows the variation with transverse distance from the path of  $\Delta A$  for different values of removed charge  $Q = 25, 150,$  and  $200$ . For this purpose, we consider the changes in ionospheric conductivity only due to the ionization changes in Figure 10, assuming that the enhanced electron temperatures last only as long as the QE fields, or typically less than a second. The transverse (or radial) variations of the disturbances are approximated with Gaussian functions, i.e.,  $e^{-(4r^2/a^2)}$ , with effective diameter  $a$  chosen to fit the radial distributions predicted with the QE model (Figure 10).

Direct comparison of the computed  $\Delta A$  values with those measured is difficult since the absolute values of the subionospheric VLF amplitude changes depend on the ambient nighttime electron density profile everywhere along the propagation path [Poulsen *et al.*, 1993a]. For relatively short ( $< 3000$  km) paths such as NLK-HU, the signal at the receiver typically consists of a superposition of several waveguide modes; if the receiver is located near a null in the amplitude pattern along the propagation path, the sensitivity of the signal amplitude to changes in the ionization profile in a localized region is substantially enhanced [Poulsen *et al.*, 1993a]. Since the locations of the nulls depend on the ambient nighttime electron density, it is difficult to make useful comparisons between predicted and measured  $\Delta A$  values without complete knowledge of the electron density at the time of the measurement.

The one aspect of our experimental findings that can be readily compared with theoretical predictions is the proximity requirement, that is, the fact that both the short duration events and the early/fast events are detected when the causative CG discharges are within  $\pm 50$  km of the path. Theoretical work indicates that the width of the scattering pattern of typical localized ionospheric disturbances does not depend sensitively on



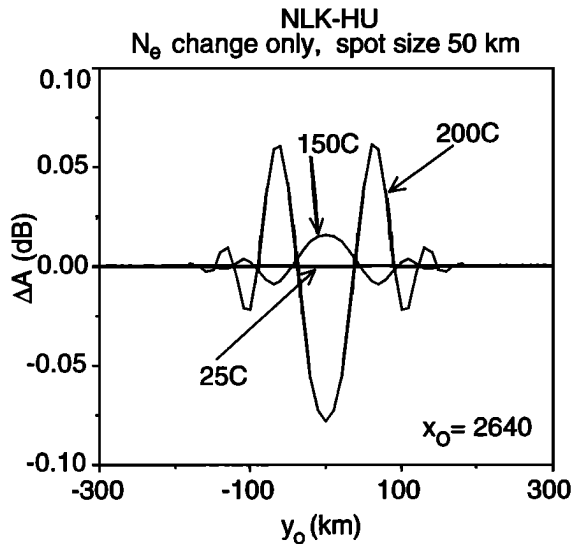


**Figure 11.** Results of a three-dimensional VLF Earth-ionosphere waveguide propagation and scattering model [Poulsen *et al.*, 1993a, b] calculations of amplitude changes of NLK-HU signal as a function of transverse distance  $y_o$  to the great circle path. The disturbance is assumed to have a Gaussian shape (i.e.,  $e^{-(4r/a)^2}$ ) in the transverse direction ( $r$ ), with the transverse size and the altitude profile of ionization as predicted by QE heating and as given in Figure 10.

the altitude profile of conductivity change but is largely determined by the transverse extent of the disturbance [Poulsen *et al.*, 1993b]. From this point of view, the results shown in Figure 11 are inconsistent with our experimental findings. For both the  $Q=150$  C and  $Q=200$  C cases, perturbations of similar amplitudes should have been observed for CG flash locations within  $\pm 100$  km of the NLK-HU path, whereas the experimental result in Figure 8, and similar observations reported earlier [Inan *et al.*, 1993], imply that only CG flashes within  $\pm 50$  km of the path should lead to detectable events. In other words, it appears that the transverse size of the ionization changes produced by the QE heating mechanism are not consistent with the data in hand.

To assess the disturbance size that is implied by the experimentally determined  $\pm 50$  km proximity requirement, we can examine the VLF diffraction pattern for the observation geometry at hand. Figure 12 shows the computed amplitude change  $\Delta A$  (in decibels) of the NLK-HU signal as a function of disturbance location transverse to the path and for different disturbance sizes. For the sake of simplicity, the disturbance is assumed to have a Gaussian shape in the radial direction (i.e.,  $e^{-(4r/a)^2}$ ) and the altitude profile of electron density within the disturbance is chosen to be that corresponding to the disturbed ionization profile for  $Q=150$  C as shown in Figure 10.

The result shown in Figure 12 indicates that ionospheric ionization disturbances involved in the case considered here may have had transverse extents of  $a \simeq 100$ -

150 km. Smaller disturbance sizes (e.g., 50-km) are not likely since disturbances at distances of 100-km would then have led to  $\Delta A$  values comparable to flashes located on the path, due to the prominent side lobes produced by the small disturbance. Similarly, disturbance sizes  $> 150$  km (e.g., 250 km) are not likely since the main beam of the pattern would have been wide enough to include the more distant CG flashes.

The transverse extent of the electron density changes are relatively small due to the highly nonlinear threshold-like dependence of the dissociative attachment and impact ionization processes on the QE field intensity. The electron temperature increases, on the other hand, can occur over much larger regions, and even relatively small amounts of charge removal (e.g.,  $Q=25$  C in Figure 10a) can lead to substantial increases (i.e., by a factor of  $> 10$  at altitude below 85 km) in electron temperature (or  $\nu_{\text{eff}}$ ), as shown in Figure 10a. Proper estimation of the transverse size of the heating region with our two dimensional QE heating model requires a prohibitively large simulation-box size. However, simpler models [Rodriguez *et al.*, 1992b] and analytical estimates (using the  $r^{-3}$  radial dependence of the primary QE fields) indicate that the transverse extent of the heating region could be as large as 200 km. Disturbances of such extent can easily lead to detectable VLF perturbations, even in the case of relatively mild heating, involving substantially smaller (tens of percent) changes in effective collision frequency, as produced by VLF transmitters [Rodriguez *et al.*, 1994]. However, it is important to note that the elevated temperatures last only as long as the QE fields, or few seconds at

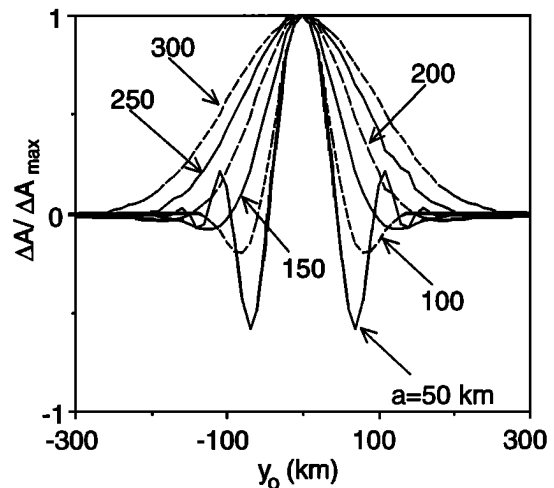


**Figure 12.** VLF diffraction pattern. The predicted variation of the change in the amplitude of the NLK signal as would be observed at Huntsville due to the appearance of a disturbance having a Gaussian shape ( $e^{-(2r/a)^2}$ ) in the radial direction, for different values of  $a$ , and as a function of the transverse distance  $y_o$  between the center of the disturbance and the VLF path.

the most. It is thus highly likely that the short duration events are simply VLF signatures of heating by QE fields in cases when the heating is not intense enough to lead to ionization changes. The large transverse extent of the disturbed region would lead to narrow diffraction pattern, consistent with the fact that the short-duration events are associated with CG flashes within  $\pm 50$  km of the 48.5-HU path (Figure 8). However, longer lasting amplitude changes (i.e., the bulk of the "early/fast" events, are clearly not likely to be due only to QE heating. The postonset peaks, on the other hand, may represent the transformation of the disturbance from one which is characterized by both a density change  $\Delta N_e$  and collision frequency change  $\Delta \nu_{\text{eff}}$  to one which involves only an ionization change  $\Delta N_e$ .

### Comparison with *Dowden et al.* [1994]

The short-duration events illustrated and discussed are similar in terms of their temporal signatures to the "rapid onset, rapid decay" phase and amplitude VLF perturbations reported by *Dowden et al.* [1994]. These authors observed VLF perturbation events that exhibited "rapid decay" ( $\sim 1$  s) and interpreted these as being due to VLF echoes from vertical columns of ionization at around 40 km altitude and having horizontal dimensions of 1-2 km and vertical dimensions of some tens of kilometers. However, there are differences in the experimental setup and the data utilized in our paper and that used by *Dowden et al.* [1994], as well as important differences in the interpretation of these events.

One difference between the two experiments is the fact that our data has an inherent time resolution of 20 ms, whereas that of *Dowden et al.* [1994] is 400 ms. The 1:20 difference in time resolution is important in establishing the simultaneity between the causative sferics and the event onsets. In our analysis, the simultaneity of occurrence (within the same 20-ms) of the sferic and event onset is the only means of identifying these events as "early", distinct from LEP events (or classic Trimp events), in which the perturbation onset is expected to be delayed with respect to the causative sferic by  $\sim 300$  ms [*Chang and Inan*, 1985] at the  $L$  shell of the NWC-Dunedin path studied by these authors. In other words, 100% of our events are accompanied by clear, distinct sferics occurring within 20-ms of the event onsets. In the *Dowden et al.* [1994] experiment, the association with sferics is only established on a statistical basis, and only 60% of their events have associated sferics. On the other hand, the time resolution available to *Dowden et al.* [1994] was well sufficient to establish the "rapid decay" nature of these events, which recover to preevent levels in  $\sim 1$  s.

The other important difference between the two experiments is the fact that we use a completely independent and definitive data set (i.e., NLDN data) to identify the time of occurrence, intensity and location

of lightning discharges. Note that most of the short duration events occurred simultaneously with NLDN recorded CG lightning flashes, occurring within  $\pm 50$  km of the VLF great circle path. We thus have clear and unambiguous association of every short duration event with both a sferic in our own receiver and CG lightning detected by the NLDN system. The "simultaneity" is established to the resolution of the measurement, which in our case is  $\pm 10$ -ms.

Our most important experimental finding, specifically the requirement of the  $\pm 50$  km proximity of the CG lightning to the affected great circle path, is inconsistent with the interpretation by *Dowden et al.* [1994] of these events as being due to scattering from 1-2 km wide ionization columns. Even if the magnitude of the scattered signal was sufficiently large, the scattering of a VLF signal (with wavelength of  $\sim 10$  km) from such an object would be nearly isotropic, so that one would see events when the CG lightning was well off from the perturbed signal path. In contrast, our interpretation of the short duration events as being due to electron temperature changes is quite consistent with the proximity requirement, as discussed in our theoretical modeling section. Note that this proximity requirement was also found to be a prominent feature of a smaller data set, reported in our earlier paper [*Inan et al.*, 1993].

### Summary

Early/fast VLF/LF perturbations provide strong evidence of the disturbance of the mesosphere/ lower ionosphere overlying thunderstorm centers for extended periods, typically for many hours.

Events are observed primarily when the VLF/LF path is within 50 km of the causative lightning discharges, indicating that the size of the disturbed ionospheric region is  $\sim 100$ -150 km. Because no other feature distinguishes the causative discharges from others, the data strongly suggests that many of the other lightning discharges not near the path must also have produced similar ionospheric disturbances, which were not detectable on the particular VLF/LF path monitored.

In addition to typical early/fast VLF/LF signatures that were previously reported, two other types of VLF/LF signatures are observed in the present data: (1) a postonset peak lasting for 1-2 s, after which the signal amplitude decreases to a new level and recovers back to preevent levels in  $\sim 100$  s. (2) short-duration events in which the entire signal amplitude change lasts only for 1-2 s. The latter type of events were most clear on the LF 48.5-kHz signal and are likely similar to the rapid onset, rapid decay events reported earlier [*Dowden et al.*, 1994]. Both the postonset peaks and the short-duration events are consistent with expected VLF/LF responses to electron temperature changes due to heating by QE fields, since the enhanced electron temperature is expected to last only as long as the QE fields, typically less than few seconds.

The amplitude changes which recover over a longer time period of  $\sim 10$ -100 s are interpreted to be due to ionization changes (either increases or decreases) caused by QE or EMP fields produced by lightning discharges. Such ionization changes would recover over timescales of  $\sim 10$ -100 s [Pasko and Inan, 1994], as observed. However, the transverse size of the ionization regions produced by QE heating is not consistent with the requirement of the causative CG flashes to be within  $\pm 50$  km of the affected paths. It is possible that the observed VLF/LF events are due to combined effects of the QE and EMP fields, or other effects of the thundercloud electric fields on the lower ionospheric and mesospheric electrons.

**Acknowledgments.** This work was supported by the National Science Foundation and the Office of Naval Research under grants NSF-ATM-9113012 and N00014-94-1-0100 to Stanford University. We greatly appreciate discussions with colleagues in the STAR Laboratory. J. V. Rodriguez was supported during this work, first by a NASA Graduate Student Researchers Program fellowship at Stanford, then by a National Research Council/AFOSR Research Associateship at Phillips Laboratory. We thank V. Idone of State University of New York for providing the NLDN data.

The Editor thanks J. R. Wait and two other referees for their assistance in evaluating this paper.

## References

- Brook, M., M. Nakano, P. Krehbiel, and T. Takeuti, The electrical structure of the Hokuriku winter thunderstorms, *J. Geophys. Res.*, **87**, 1207, 1982.
- Budden, K. G., *The Wave-guide Mode Theory of Wave Propagation*, Prentice-Hall, Englewood Cliffs, N. J., 1961.
- Chang, H. C., and U. S. Inan, Lightning-induced electron precipitation from the magnetosphere, *J. Geophys. Res.*, **90**, 1531, 1985.
- Davies, K., *Ionospheric Radio*, Peter Peregrinus, London, 1990.
- Dejnakarintra, M., and C. G. Park, Lightning-induced electric fields in the ionosphere, *J. Geophys. Res.*, **79**, 1903, 1974.
- Dowden, R. L., C. D. D. Adams, J. B. Brundell, and P. E. Dowden, Rapid onset, rapid decay (RORD), phase and amplitude perturbations of VLF subionospheric transmissions, *J. Atmos. Terr. Phys.*, **56**(11), 1513, 1994.
- Fishman, G. J., P. N. Bhat, R. Mallozzi, J. M. Horack, T. Koshut, C. Kouveliotou, G. N. Pendleton, C. A. Meegan, R. B. Wilson, W. S. Paciesas, S. J. Goodman, and H. J. Christian, Discovery of intense gamma-ray flashes of atmospheric origin, *Science*, **264**, 1313, 1994.
- Holzworth, R. H., M. C. Kelley, C. L. Siefring, L. C. Hale, and J. T. Mitchell, Electrical measurements in the atmosphere and the ionosphere over an active thunderstorm, 2, Direct current electric fields and conductivity, *J. Geophys. Res.*, **90**, 9824, 1985.
- Idone, V.P., A.B. Saljoughy, R. W. Henderson, P. K. Moore, and R. B. Pyle, A reexamination of the peak current calibration of the National Lightning Detection Network, *Geophys. Res. Lett.*, **98**, 18323, 1993.
- Inan, U. S., D. L. Carpenter, R. A. Helliwell, and J. P. Katsufakis, Subionospheric VLF/LF phase perturbations produced by lightning-whistler induced particle precipitation, *J. Geophys. Res.*, **90**, 7457, 1985.
- Inan, U. S., D. C. Shafer, W. Y. Yip, and R. E. Orville, Subionospheric VLF signatures of nighttime *D*-region perturbations in the vicinity of lightning discharges, *J. Geophys. Res.*, **93**, 11455, 1988.
- Inan, U. S., T. F. Bell, and J. V. Rodriguez, Heating and ionization of the lower ionosphere by lightning, *Geophys. Res. Lett.*, **18**, 705, 1991.
- Inan, U. S., J. V. Rodriguez, and V. P. Idone, VLF signatures of lightning-induced heating and ionization of the nighttime *D*-region, *Geophys. Res. Lett.*, **20**, 2355, 1993.
- Lyons, W. A., Characteristics of luminous structures in the stratosphere above thunderstorms as imaged by low-light video, *Geophys. Res. Lett.*, **21**, 875, 1994.
- Orville, R. E., Calibration of a magnetic direction finding network using measured triggered lightning return stroke peak currents, *J. Geophys. Res.*, **96**, 17135, 1991.
- Orville, R. E., R. A. Weisman, R. B. Pyle, R. W. Henderson, and R. E. Orville Jr., Cloud-to-ground lightning flash characteristics from June 1984 through May 1985, *Geophys. Res. Lett.*, **92**, 5640, 1987.
- Pasko, V.P., and U. S. Inan, Recovery signatures of lightning-associated VLF perturbations as a measure of the lower ionosphere, *J. Geophys. Res.*, **99**, 17523, 1994.
- Pasko, V. P., U. S. Inan, Y. N. Taranenko, and T. F. Bell, Heating, ionization and upward discharges in the mesosphere due to intense quasi-electrostatic thundercloud fields, *Geophys. Res. Lett.*, **22**, 365, 1995.
- Poulsen, W. L., U. S. Inan, and T. F. Bell, A multiple-mode three-dimensional model of VLF propagation in the earth-ionosphere waveguide in the presence of localized *D* region disturbances, *J. Geophys. Res.*, **98**, 1705, 1993a.
- Poulsen, W. L., T. F. Bell, and U. S. Inan, The scattering of VLF waves by localized ionospheric disturbances produced by lightning-induced electron precipitation, *J. Geophys. Res.*, **98**, 15553, 1993b.
- Rodriguez, J. V., U. S. Inan, Y. Q. Li, R. H. Holzworth, A. J. Smith, R. E. Orville, and T. J. Rosenberg, A case study of lightning, whistlers, and associated ionospheric effects during a substorm particle injection event, *J. Geophys. Res.*, **97**, 65, 1992a.
- Rodriguez, J. V., U. S. Inan and T. F. Bell, *D* region disturbances caused by electromagnetic pulses from lightning, *Geophys. Res. Lett.*, **19**, 2067, 1992b.
- Rodriguez, J. V., Umran S. Inan, and T. F. Bell, Heating of the nighttime *D* region by very low frequency transmitters, *J. Geophys. Res.*, **99**, 23329, 1994.
- Sentman, D. D., and E. M. Wescott, Observations of upper atmospheric optical flashes recorded from an aircraft, *Geophys. Res. Lett.*, **20**, 2857, 1993.
- Sentman, D. D., E. M. Wescott, D. L. Osborne, D. L. Hampton, M. J. Heavner, Preliminary results from the Sprites94 campaign: Red sprites, *Geophys. Res. Lett.*, **22**, 1205, 1995.

- Taranenko, Y. N., U. S. Inan, and T. F. Bell, The interaction with the lower ionosphere of electromagnetic pulses from lightning: Heating, attachment, and ionization, *Geophys. Res. Lett.*, *20*, 1539, 1993.
- Uman, M.A., *The Lightning Discharge*, Academic, San Diego, Calif., 1987.
- Wait, J. R., and K. P. Spies, Characteristics of the Earth-ionosphere waveguide for VLF radio waves, *Tech. Note 300*, Nat. Bur. of Stand., Washington, D. C., 1964.
- Wescott, E. M., D. Sentman, D. Osbarne, D. Hampton, and M. Heavner, Preliminary results from the Sprites 94 Campaign: Blue jets, *Geophys. Res. Lett.*, *22*, 1209, 1995.
- 
- U.S. Inan and V.P. Pasko, STAR Laboratory, Stanford University, Stanford, CA 94305.
- J.V. Rodriguez, Ionospheric Effects Division, Phillips Laboratory, Hanscom Air Force Base, MA 01731.
- A. Slingeland, Qualcomm Inc., 5565 Morehouse Drive, San Diego, CA 92121-1710.

(Received July 13, 1995; revised November 14, 1995; accepted November 14, 1995.)